Acta Crystallographica Section D
Biological Crystallography
ISSN 0907-4449

Crystallization and preliminary diffraction data analysis of both single and pseudo-merohedrally twinned crystals of rubredoxin oxygen oxidoreductase from *Desulfovibrio gigas*

C. Frazão,[a] L. Sieker,[a] R. Coelho,[a] J. Morais,[a] I. Pacheco,[a] L. Chen,[b] J. LeGall,[b] Z. Dauter,[c] K. Wilson[c] and M. A. Carrondo[a]*

[a]Instituto de Tecnologia Química e Biológica, Apartado 127,2780-Oeiras, Portugal, [b]Department of Biochemistry, University of Georgia, Athens, Georgia 30602, USA, and [c]European Molecular Biology Laboratory, c/o DESY, Notkestrasse 85, 22603 Hamburg, Germany

Correspondence e-mail: carrondo@itqb.unl.pt

Received 1 April 1999
Accepted 4 May 1999

Crystals of rubredoxin oxygen oxidoreductase have been obtained and characterized. They belong to space group $P2_12_12$, with unit-cell dimensions a = 88.24 (15), b = 101.25 (7), c = 90.80 (3) Å. The homodimer (86 kDa) in the asymmetric unit is related by a non-crystallographic twofold rotation axis parallel to the *ab* 'diagonal' direction, as shown by the self-rotation maximum in the section with $\chi = 180^\circ$. This pseudo-crystallographic symmetry element was also found to be the twinning axis of pseudo-merohedrally twinned crystals, leading to apparent pseudo-tetragonal $P42_12$ crystal symmetry.

1. Introduction

Desulfovibrio gigas is a sulfate-reducing bacterium which is able to utilize polyglucose for the formation of ATP associated with the reduction of dioxygen to water (Santos *et al.*, 1995). Rubredoxin oxygen oxidoreductase (ROO), an 86 kDa homodimer (Chen *et al.*, 1993*a*), is the terminal element of a soluble electron-transfer chain in *D. gigas*, where electrons flow from NADH to oxygen through NADH-rubredoxin oxidoreductase (Chen *et al.*, 1993*b*) and rubredoxin (LeGall & Dragoni, 1996). ROO contains flavin as a prosthetic group (Timkovich *et al.*, 1994). Spectroscopic studies (Gomes *et al.*, 1997) showed that the flavins accept electrons from rubredoxin. These data have been further supported by the finding that rubredoxin and ROO are located in the same polycistronic unit of the *D. gigas* genome. However, since the direct reduction of oxygen to water by flavins is unprecedented, the presence of another redox centre, as yet undetected, cannot be ruled out.

A twinned crystal consists of a specimen containing two or more single crystals of the same species, but in different orientations (Koch, 1995). In contrast to epitaxic twins, in which the twin components have unrelated orientations and therefore produce rotational images showing the superposition of their lattices, merohedral twins are formed by domains whose lattices overlap perfectly in three dimensions. Their diffraction patterns seem to be that of a single crystal, but the observed diffraction data do not represent the true crystallographic intensities: each spot is an overlap of different reflections from the different domains (which coincide because the twinning operator belongs to the underlying apparent crystal point group). Cases where the lattices of the different components overlap approximately (but not exactly) in three dimensions owing to fortuitous unit-cell geometry are referred as pseudo-merohedral. The crystal intensity distribution (Wilson, 1949) is smoothed by the fact that each observed intensity is a weighted average, over the twin domains, of the (pseudo) overlapping reflections. Twinning can, therefore, be recognized or diagnosed by inspection of the intensity distribution statistics (Rees, 1980). In principle, twins can be composed by several twin domains, but for proteins it seems that only cases with two twin domains have been reported – cases of hemihedral twinning (Yeates, 1997). When the two domains have the same global volume and contribute equally to the total diffraction power of the crystal, the twinning is usually called 'perfect'.

In this work, we report the crystallization of ROO samples and present a preliminary crystallographic analysis of the crystals obtained.

2. Materials and methods

2.1. Protein crystallization

Purified native ROO was obtained as described by Chen *et al.* (1993*a*). Screening for crystallization conditions indicated that ROO crystallizes by vapor diffusion at room temperature in the pH range 5–9, using polyethylene glycols (PEGs) in the molecular-weight range 1–6 K as precipitating agents. Crystals appear within 1 d, mostly in very large numbers, together with a gelatinous precipitate from which they are difficult to separate. The gelatinous precipitate, however, can be avoided by lowering the temperature and/or by addition of a detergent additive, SB12 (*N*-dodecyl-*N*,*N*-dimethyl-3-ammonio-1-propanesulfonate, Sigma Chemical Co.). In a typical crystallization trial, a sitting drop consisting of

Table 1
Crystallographic statictics of rubredoxin oxygen oxidoreductase.

	Crystal *A*	Crystal *B*	Crystal *C*	Crystal *D*
Crystal growing conditions	Room temperature (no detergent)	Cold room	Cold room	Cold room
X-ray source (wavelength in Å)	EMBL, X11 (0.92)	Enraf–Nonius 4.5 kW (1.5418)	EMBL, X31 (1.4)	Enraf–Nonius 4.5 kW (1.5418)
Crystal dimensions (mm)	0.4, 0.2, 0.2	0.25, 0.12, 0.07	0.17, 0.17, 0.17	0.18, 0.18, 0.15
Data-collection temperature (K)	278	115	120	105
Mosaicity (°)	0.29–0.52	0.43–0.49	0.66–1.08	0.43–0.56
Unit-cell dimensions (Å)	98.24 (15), 101.25 (7), 90.80 (3)	98.54 (3), 98.89 (3), 90.62 (3)	98.58 (10), 98.82 (6), 90.62 (2)	98.69 (4), 98.72 (4), 90.66 (6)
Resolution (Å)	29.4–2.5	24.9–2.9	29.5–2.3	31.6–2.9
Total rotation scan (°)	95.0	94.2	137.2	217.7
Processed intensities	123925	76002	169486	175556
Unique intensities	33826	18768	37023	20265
Redundancy	3.5	4.0	4.6	8.7
Completeness (%)	99.6	92.8	92.5	99.9
$I > 3\sigma(I)$ (%)	81.3	83.7	90.3	97.7
$I/\sigma(I)$	17.5	10.9	13.7	24.0
$R_{\rm merge}(I)$ (%) (for putative space group $P42_12$)	6.6	12.2 (42.2)	9.6 (24.8)	8.3 (10.4)
Completeness (%) (outer shell†)	96.9	93.1	83.8	99.9
$I/\sigma(I)$ (%) (outer shell†)	4.3	3.0	5.1	9.7
$R_{\rm merge}$ (*I*) (%) (outer shell†)	26.9	30.5	25.9	18.5
Centric $\lvert E^2 - 1\rvert$‡ zones 0*kl*, *h*0*l*, *hk*0	1.002, 1.014, 0.999	0.905, 0.944, 0.869	0.753, 0.836, 0.788	0.764, 0.784, 0.739
Acentric $\lvert E^2 - 1\rvert$‡	0.759	0.690	0.603	0.573

† Outer shell (Å): crystal *A*, 2.49–2.45; crystal *B*, 2.95–2.90; crystal *C*, 2.34–2.30; crystal *D*, 2.94–2.89. ‡ The theoretical values for $\lvert E^2 - 1\rvert$ in single crystals with a random distribution of atoms are 0.968 for centric reflections and 0.736 for acentric reflections.

3 µl of precipitant solution and 3 µl of protein solution (10 mg ml^{-1}) was deposited on a microbridge from DROP (Devis Realisation Outillage Precision, Grenoble) and equilibrated against precipitant solution consisting of 10%(*v*/*v*) PEG 6K buffered at pH 6.0 by Tris-maleic acid 100 m*M*, in a well of a Linbro box (Flow Laboratories, Inc., McLean, VA).

Cryo-stabilization of the crystals was only possible if performed in the cold room and in a very slow process. The well solution was replaced by the final cryo-protection solution, which consisted of the previously described precipitant solution complemented with glycerol to a final concentration of 25%(*v*/*v*). Precipitant solution was added to the sitting drops containing the crystals until a total volume of about 20 µl was reached. The cryo-protection solution was then added in minute amounts (*ca* 0.2 µl) to the drops and was allowed to diffuse through the mother liquor and crystals. A faster increase in glycerol concentration invariably led to rupture of the crystals. The crystal cryo-stabilization proceeded over 2 d, until a final concentration of 25% glycerol was reached.

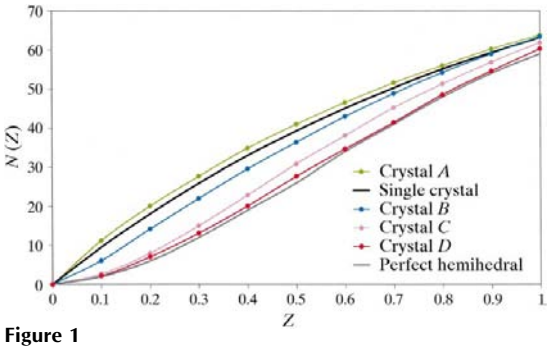

Figure 1
Acentric cumulative Wilson distribution of crystal intensities. The theoretical distributions for a single crystal and for a perfect hemihedral twin are shown, together with the distributions from several ROO crystals (see Table 1). ROO crystals grown at room temperature (crystal *A*) seemed identical to those grown in the cold (crystals *B*, *C* and *D*). However, the intensity distributions of the latter showed a sigmoidal shape below that of a theoretical single crystal.

2.2. Crystallographic diffraction data collection and processing

Diffraction data from crystals grown at ambient or cold-room temperatures were obtained using an Enraf–Nonius FR570 rotating-anode generator operating at 4.5 kW with a Huber graphite monochromator to select Cu $K\alpha$ radiation, or using synchrotron radiation at stations X31 and X11 of DESY, EMBL Outstation, Hamburg. Cryo-conditions were used for some of the data-collection experiments, using an Oxford Cryosystems Cryostream. Data were collected on image-plate devices from MAR Research and were processed with the *DENZO*/*SCALEPACK* (Otwinowski & Minor, 1997) suite of programs. The *CCP*4 package (Collaborative Computational Project, Number 4, 1994) was used to calculate observed structure factors and their intensity distribution (*TRUNCATE*), to normalize them (*ECALC*) and to calculate the self-rotation function (*POLARRFN*). *SHELXS* (Sheldrick, 1997) was used to calculate a twinning diagnostic parameter, $\langle\lvert E^2 - 1\rvert\rangle$. Table 1 indicates the data-collection conditions and statistics for the different diffraction data sets.

3. Results and discussion

3.1. Crystal data

ROO orange–brown crystals have a parallelepiped shape and have relative dimensions which vary from specimen to specimen. In favorable cases, they can reach 0.2–0.4 mm in their largest dimension within three weeks.

The crystals belong to space group $P2_12_12$, with unit-cell dimensions a = 98.24 (15), b = 101.25 (7), c = 90.80 (3) Å for the best single-crystal data set collected thus far (crystal *A* in Table 1). When grown at room temperature, a gel-like precipitate develops during crystallization, which makes crystal handling difficult. On the other hand, if crystals are grown in the cold and/or with addition of detergent, the gel-like precipitate can be avoided and the number of crystals per drop controlled. The crystals' shape and color remain essentially similar to those grown at room temperature, but their diffraction data show a Wilson cumulative distribution (Fig. 1) characteristic of merohedral twinning (Rees, 1980), with a recognizable sigmoidal shape below the exponential curve for the theoretical single-

crystal distribution (Gomis-Rüth *et al.*, 1995). The diagnostic centric and acentric $\langle|E^2-1|\rangle$ values for the various crystals were found within the 0.740–0.973 and the 0.572–0.759 ranges; *cf.* the single-crystal values of $\langle|E^2-1|_{\rm centric}\rangle = 0.968$ and $\langle|E^2-1|_{\rm acentric}\rangle = 0.736$, expected theoretically, respectively (Wilson, 1949).

For orthorhombic crystals, pseudo-merohedral twinning is possible in the case of degeneracy of the *a* and the *b* dimensions, which leads to a pseudo-tetragonal lattice. Additionally, an apparent symmetry increase in the intensity distribution from the orthorhombic to the tetragonal system will occur if the *ab* diagonal is a twofold twinning axis. This will be fully accomplished in the case where the ratio between the two twin components reaches 0.5:0.5. In fact, for all cold-room-grown ROO crystals, there was shrinkage of the *b* axis towards the *a*-axis dimension, resulting in an 'almost tetragonal' lattice, with the twofold twinning axis lying along the *ab* 'diagonal'. The relative intensity distribution was then altered, and eventually (crystal *D*, last column in Table 1) displayed a pseudo-tetragonal $P42_12$ system. Details and statistics of the different diffraction data sets are given in Table 1.

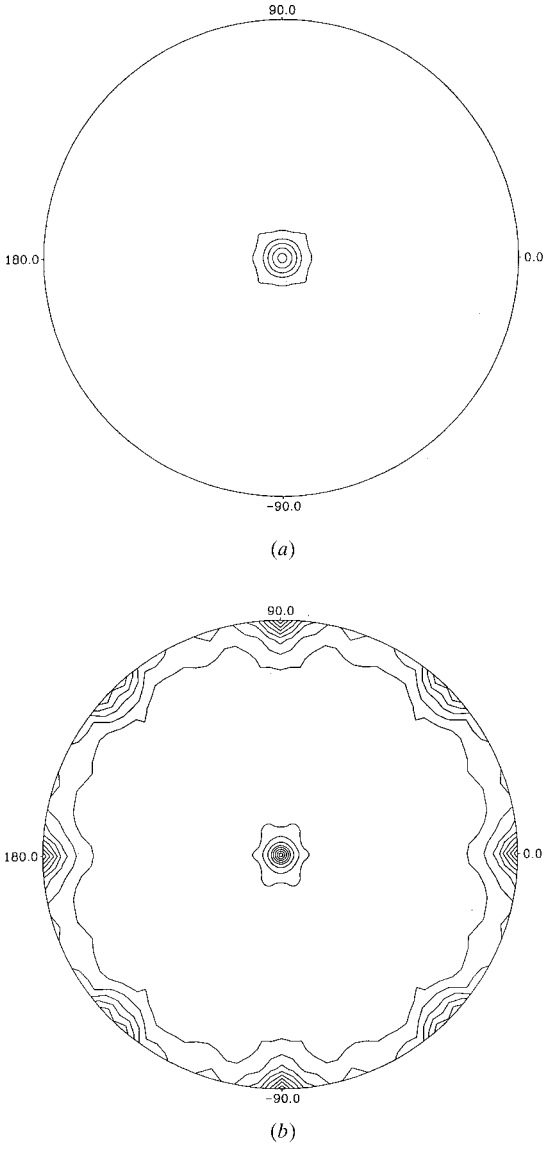

Figure 2
Self-rotation function maps of ROO for (*a*) the $\chi = 85^\circ$ section and (*b*) the $\chi = 180^\circ$ section. Non-crystallographic symmetry is recognized by peak heights of 69% of the origin peak. The pseudo-fourfold rotation axis (*a*) is parallel to *c*, with its maximum at $\chi = 84.1^\circ$; the twofold rotation axis (*b*) lies at $\varphi = 42.9$, $\omega = 90.0^\circ$. Map contouring is at 1σ.

3.2. Cryo-protection

The cryo-protection of ROO crystals was a delicate procedure. Success could only be achieved when a very slow approach was tried in the cold room, as described in §2.1. If the addition of cryo-protectant was too fast, the crystals would typically start to fracture, beginning at the side with higher glycerol concentration. The diffraction properties (resolution and precision, as well as crystal stability) improved markedly by the use of cryo-techniques. At room temperature with a rotating-anode source, data were not better than 3.5 Å, $R_{\rm merge} = 13\%$ (C. Frazão, data not shown). At 278 K and using synchrotron radiation, data were collected to 2.5 Å, $R_{\rm merge} = 6.6\%$ (crystal *A* in Table 1). This compares favorably with data collected under cryo-conditions and with a rotating-anode source: 2.9 Å resolution, $R_{\rm merge} = 12.2$ and 8.3% (for crystals *B* and *D* in Table 1, respectively).

3.3. Pseudo symmetry

The calculated solvent content (Matthews, 1968) for the single orthorhombic crystals is 52%, assuming a protein homodimer in the asymmetric unit.

Self-rotation calculations, using normalized structure factors for the single-crystal diffraction data, indicated strong non-crystallographic symmetry features at the $\chi = 180^\circ$ and near the $\chi = 90^\circ$ sections (Figs. 2*a* and 2*b*). A strong peak at $\omega = 90.0$, $\varphi = 42.9$, $\chi = 180^\circ$ with an intensity height of 69% of the origin indicates a non-crystallographic twofold axis parallel to the pseudo-diagonal between axes *a* and *b* (their relative dimensions differ by only *ca* 3%). The association of this non-crystallographic twofold rotation axis with the crystallographic orthorhombic symmetry produces an almost fourfold non-crystallographic symmetry axis parallel to axis *c* (detected at $\omega = 0.0$, $\varphi = 176.8$ or 12.7°, $\chi = 85.8$ or 94.2°). The observed twinning in ROO crystals therefore seems reminiscent of the pseudo-symmetry within the asymmetric unit.

We thank the staff of the University of Georgia for growing the bacteria, and Dr M.-Y. Liu for assisting in the protein purification. This work was supported by grant GM56001-02 from the National Institute of Health and grants PRAXIS/PCNA/C/BIO/0076/96 and PRAXIS/2/2.1/QUI/17/94 from Junta Nacional de Investigação Científica, and European Union TMR Project ERBFMGECT980134.

References

Chen, L., Liu, M.-Y., LeGall, J., Fareleira, P., Santos, H. & Xavier, A. V. (1993*a*). *Biochem. Biophys. Res. Commun.* **193**, 100–105.
Chen, L., Liu, M.-Y., LeGall, J., Fareleira, P., Santos, H. & Xavier, A. V. (1993*b*). *Biochem. Biophys. Res. Commun.* **216**, 443–448.
Collaborative Computational Project, Number 4 (1994). *Acta Cryst.* D**50**, 760–763.
Gomes, C. H., Silva, G., Oliveira, R., LeGall, J., Liu, M.-Y., Xavier, A. V., Rodrigues-Pousada, C. & Teixeira, M. (1997). *J. Biol. Chem.* **272**, 22502–22508.
Gomis-Rüth, F. X., Fita, I., Kiefersauer, R., Huber, R., Avilés, F. X. & Navaza, J. (1995). *Acta Cryst.* D**51**, 819–823.
Koch, E. (1995). In *International Tables for Crystallography*, Vol. C, edited by A. J. C. Wilson. Dordrecht: Kluwer Academic Publishers**.**
LeGall, J. & Dragoni, N. (1996). *Biochem. Biophys. Res. Commun.* **23**, 145–149.
Matthews, B. W. (1968). *J. Mol. Biol.* **33**, 491–497.
Otwinowski, Z. & Minor, W. (1997). *Methods Enzymol.* **276**, 307–326.
Rees, D. C. (1980). *Acta Cryst.* A**36**, 578–581.
Santos, H., Fareleira, P., Xavier, A. V., Chen, L., Liu, M.-Y. & LeGall, J. (1995). *Biochem. Biophys. Res. Commun.* **195**, 551–557.
Sheldrick, G. M. (1997). *Methods Enzymol.* **276**, 628–641.
Timkovich, R., Burkhalter, R. S., Xavier, A. V., Chen, L. & LeGall, J. (1994). *Bioorg. Chem.* **22**, 284–293.
Wilson, A. J. C. (1949). *Acta Cryst.* **2**, 318–321.
Yeates, T. O. (1997). *Methods Enzymol.* **276**, 344–358.